

# Quantifying the Impact of Localization Error on Indoor Channel Prediction Using REMs

Friedrich Burmeister<sup>1</sup>, Zhongju Li<sup>1</sup>, Nick Schwarzenberg<sup>1</sup>, Andreas Traßl<sup>1,2</sup>, Richard Jacob<sup>1</sup>, and Gerhard Fettweis<sup>1,2</sup>

<sup>1</sup>Vodafone Chair Mobile Communications Systems, Technische Universität Dresden, Germany

<sup>2</sup>Centre for Tactile Internet with Human-in-the-Loop (CeTI)

{friedrich.burmeister, zhongju.li, nick.schwarzenberg, andreas.traßl, richard.jacob, gerhard.fettweis}@tu-dresden.de

**Abstract**—Knowledge about the current and future states of a radio channel takes the reliability of a communications system to a new level. A Radio Environment Map (REM) contains information about the channel state in the spatial domain for a given environment. Given a known user trajectory, this information can be used for channel prediction. In this work, we investigated the two primary limitations to this approach: the required spatio-temporal stationarity of the channel and the high localization accuracy of the user. The channel stationarity is quantified by repeated channel measurements. The high measurable consistency indicates the value of REMs in non-changing environments. Based on a high-resolution REM that we measured in an office environment, we quantify the impact of one- and two-dimensional localization errors on the resulting prediction error. With the results shown, localization accuracy requirements can be derived given the target channel prediction accuracy. Also, the results help to determine the required spatial resolution of REM measurements in practice.

**Index Terms**—Radio Environment Maps, Radio Channel, Channel Measurements, Channel Prediction, Indoor.

## I. INTRODUCTION

Thanks to current radio technologies, e.g., 5G, an ongoing automation of industrial factories and warehouses with autonomous robots can be observed. Thereby, the remote control of robots, e.g., of single Automated Guided Vehicles (AGVs) or of AGV fleets for cooperative transports, is an important use case for wireless communications in an industrial context [1]. Such closed-loop control systems have tight requirements regarding latency and reliability, which can be served by Ultra-Reliable Low-Latency Communications (URLLC) [2].

As a consequence of mobility, industrial robots experience a time-varying radio channel. The time-varying attenuation of radio signals by the channel is one cause for communication outages as a consequence of insufficient receive power. With explicit knowledge of the radio channel conditions as well as future channel states, reliability-increasing measures can be taken to prevent such outages. A possible approach could be to temporarily increase the transmit power or to adapt the Modulation Coding Scheme (MCS) when a critical attenuation through the radio channel is imminent. To take such measures proactively, knowledge of critical channel conditions is required in advance. A possible solution is channel prediction, where the latest available channel observations are used to

extrapolate the channel into the near future [3]. On one hand, the prediction horizon, i.e., the time we can predict in the future, is limited by the temporal correlation of the radio channel. On the other hand, the higher the prediction horizon and the precision of the prediction, the more value it generates for a communications system. To overcome this limitation, we investigate to use long-term correlations in form of existing information from Radio Environment Maps (REMs) to predict the channel into the future. In sparsely changing environments, such as industrial halls, a high spatio-temporal channel stationarity, i.e., a very similar channel at the same positions over time can be observed. If a REM exists and the position of the robot is known, the channel can be predicted for future locations of the robot based on its planned trajectory. Especially in industrial environments, trajectories of AGVs are likely to repeat and to be constrained to certain areas. In addition, high-precision localization for indoor environments is a set target for 6G systems [4]. In this context, building REMs, e.g., by crowdsourcing, seems reasonable.

To assess the usability of high-resolution REMs for channel predictions, the assumption of spatio-temporal channel stationarity has to be researched first. Furthermore, since this prediction method is based on a precise localization, the impact of erroneous localization on the predictions is to be investigated. In the literature, measuring radio channels such that REMs can be constructed subsequently is a well known research problem. [5]–[7] Thereby, the main motivation behind existing work is to perform indoor localization of devices/robots using mechanisms such as fingerprinting [8], or to predict the REMs for unseen places. Little research has been conducted on approaches using existing data for indoor communications systems, especially in the context of channel prediction. In [9], the authors propose to use the knowledge about the radio environment for planning the paths of autonomous robots to optimize the receive power during the trajectory and to perform transmit power adaption based on the radio map. However, the work is restricted to simulations in a simplified radio environment. In [10], point-wise measured data is used for channel predictions. But, the influence of localization error was investigated only for a constant position error of 6 cm and the distance of measured points in space was not resulting in a high-resolution radio map.

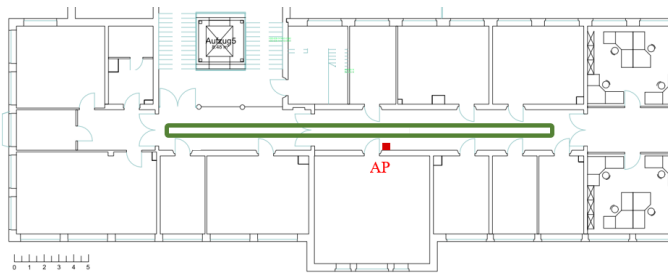


Fig. 1: Map of the office environment the AGV is moving in. The trajectory is marked in green while the position of the receiving unit is given as red square.

To address the research question whether REMs can be used for channel predictions, we present the results of a measurement campaign conducted for this purpose. Thereby, we provide the following contributions:

- Channel stationarity is shown to be a valid assumption in real-world measured channels by correlating repeated measurements.
- Based on the stationarity, we show that measuring a REM is possible with a dynamic measurement system while exceeding the spatial resolution of existing work.
- Having a channel prediction in mind, the impact of one- and two-dimensional localization errors is investigated systematically. The results serve as localization requirements needed to bound the prediction error.

## II. MEASUREMENT SYSTEM

The channel sounding system which was used to collect the measurement data was first described in [11]. A Radio Frequency (RF) transmitter is placed on top of an AGV. During the measurements, the AGV moves on a predefined trajectory and the transmitter periodically radiates a training signal, in this case a Zadoff-Chu sequence. Due to the knowledge about the training signal at the receiver, the channel impulse response (CIR) can be determined by correlating the received signal samples with the training signal. One of the main differences to the measurements performed in [11] is the measurement environment. For this work, measurements were conducted in a corridor of an office environment at Technische Universität Dresden. [12] A map of the building environment showing the surrounding rooms, the trajectory of the AGV as well as the position of the receiving point are shown in Fig. 1. The maximum usable track has an extension of more than 25 m in horizontal direction and 0.6 m in vertical direction. In this work, we utilize the track marked with a green solid line in Fig. 1. The resulting lap consists of an upper and a lower straight and has a total length of almost 70 m. The vehicle moves with a constant speed of 0.8 m/s. The omnidirectional transmit antenna on the AGV is mounted at a height of 0.5 m above the ground. Omnidirectional antennas of the same type are used for the receiving units mounted at a height of 2.5 m and are thus similar to a typical Access Point (AP) setup.

Transmitter and receiver functionalities are based on a clock-driven FPGA implementation deployed on Software-

Defined Radios (SDRs) of type USRP 2974 from *National Instruments*. Sampling is performed with a frequency of 100 MHz around a carrier frequency of 3.75 GHz. Thus, the spectrum between 3.7 GHz to 3.8 GHz for industrial campus networks is covered. Thanks to the clock-driven implementation, we are able to measure CIRs with a constant and high measurement rate of 1 kHz. Hence, the system captures one CIR per millisecond which equals a distance of 0.8 mm between consecutive measurement points. With help of a consistent measurement rate in combination with a constant motion of the measurement vehicle, we study the reproducibility of the measurements and thus how stationary the radio channel is. Thereby, we are interested in the wideband receive power in the first place. The signal receive power is computed based on the measured CIRs  $h[n]$ , where  $n$  is the delay index with  $n \in \{0, 1, \dots, N - 1\}$  and  $N = 512$ . First, the delay-domain CIR  $h[n]$  is transformed into a channel frequency response  $H[m]$  via Fast Fourier Transform (FFT), where  $m \in \{0, 1, \dots, N - 1\}$  is the index of the frequency bin in the spectrum  $H$ . The total receive power  $P_{rx}$  of the signal is calculated by summing up the squared magnitudes of all  $N$  frequency bins in the spectrum. To calculate the receive power of a dedicated band within the spectrum, e.g., reaching from bin  $M_1$  to  $M_2$ , we compute

$$P_{rx} = \sum_{m=M_1}^{M_2} |H[m]|^2 \quad . \quad (1)$$

The outer 10% of the spectrum are attenuated by hardware-related filter effects respectively. To compensate this effect, we consider the inner 400 frequency bins, i.e.,  $M_1 = 56$  and  $M_2 = 455$ , resulting in a bandwidth of  $78.125\text{MHz} \approx 80\text{MHz}$ . It has to be noted that the resulting absolute receive powers of our measurements are not subject to any calibration. Thus, the absolute level of  $P_{rx}$  is difficult to compare with other measurement systems. However, since relative level differences are not affected, this fact is no limitation for the results presented in this paper. Both, the study of stationarity and the influence of localization on prediction are based on relative differences in receive power and are thus generally valid.

The measurement data of this campaign are freely available as a data set. [13] The source code to reproduce the results is also freely available.<sup>1</sup>

## III. SPATIO-TEMPORAL CHANNEL STATIONARITY

The fundamental question driving this work is about the value of existing radio channel information for channel prediction. To address this question, we investigate the spatio-temporal stationarity of the radio channel. In other words, how similar is a real-world channel at the same local position at different points in time, e.g., if the AGV is repeating its trajectory multiple times. To answer this question, we rely on the ability of our measurement setup to reproduce consistent

<sup>1</sup><https://gitlab.vodafone-chair.org/friedrich.burmeister/impact-of-localization-error-on-rem-based-radio-channel-predictions.git>

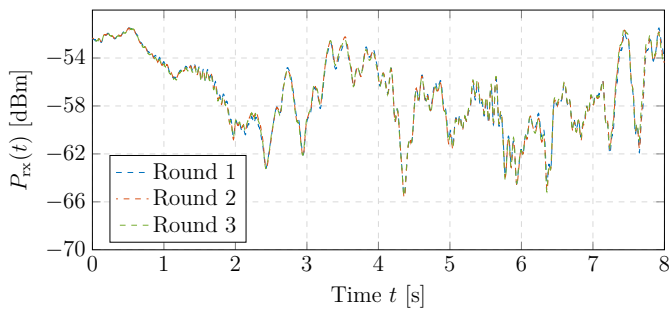


Fig. 2: Matching receive power time series of 3 consecutive measurement rounds as indicator for measurement reproducibility.

| BW [MHz] | $\rho$ | MAE [dB] | Median [dB] | Data samples |
|----------|--------|----------|-------------|--------------|
| 80       | 0.9984 | 0.179    | 0.133       | 1.59e5       |
| 40       | 0.9979 | 0.229    | 0.164       | 3.18e5       |
| 20       | 0.9971 | 0.278    | 0.192       | 6.36e5       |
| 10       | 0.9963 | 0.321    | 0.213       | 1.27e6       |
| 5        | 0.9953 | 0.358    | 0.229       | 2.54e6       |

TABLE I: Round correlations, mean deviation and median deviation between rounds compared for different bandwidths.

measurement results. The argumentation is as follows: if we are able to measure repeating results, reusing previous information about the radio environment is possible.

To assess stationarity, the AGV performed three rounds of measuring. Between each round there was a delay of two minutes. The position of the antenna on the surface of the AGV was not varied between the measurement repetitions. Furthermore, the environment remained unchanged during the measurement repetitions. To eliminate any influence of moving objects on the radio environment, such as moving persons, the measurements were conducted at night so that no people were present in the office environment.

The receive power time series from the same portion of the three rounds are depicted in Fig. 2. The receive power is determined for a bandwidth of 80 MHz. Looking at Fig. 2 already indicates the excellent consistency of delayed measurement rounds. Not only slow and large attenuations and gains of the receive power coincide, but also small and fast changes are matching. What seems like a random fluctuation recurs round after round. To quantify the consistency of the results, we compute the Pearson correlation coefficient  $\rho$  between all three rounds and determine the mean and median (50th percentile) of the absolute deviation between the time series. The results are given in Tab. I. Since we are also interested in the consistency of the frequency spectra, we compute the receive power from narrower frequency bands and evaluate the correlation and deviations between the rounds for smaller bands. The results are also given in Tab. I. Due to a growing impact of noise for smaller bandwidths, the correlation slowly degrades but is still on a very high level of 99.53% for bands with 5 MHz of bandwidth. Also the absolute deviation slowly increases but is still in a negligible order of magnitude compared to

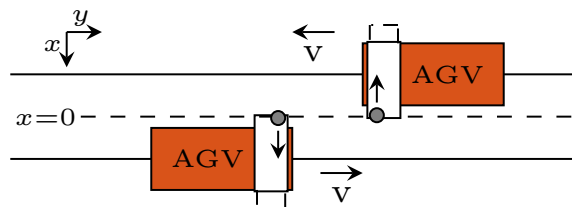


Fig. 3: Sequentially scanning the radio environment by shifting the antenna on a moving AGV

the receive power range. The data of repetitive measurements in [11] employing the same measurement system showed the same channel stationarity but in an industrial environment.

What conclusions are we able to draw from the observation that measurement results are reproducible? In the first place, the reproducibility is an indicator for the quality and accuracy of the measurement system, i.e., the motion of the vehicle as well as the sampling works reliable. It also shows that the Signal-to-Noise Ratio (SNR) is high enough during the measurements such that observed receive powers and receive power deviations are caused by the radio channel. Other influences such as measurement noise do not have a significant effect. Channel measurements are indeed reproducible and the channel is spatio-temporal stationary.

#### IV. HIGH-RESOLUTION RADIO ENVIRONMENT MAP

Due to channel stationarity, it is shown that the receive power is not varying over time at a given position in case of a static environment. This fact reinforces the value of existing channel knowledge at a given position for the aim of channel predictions. In order to allow predictions not only for a single trajectory and a single spatial direction, channel data is needed for more than just a single measured line. Instead, channel data needs to be acquired for a continuous two-dimensional area. Moreover, this is necessary if we want to study the impact of localization error in two spatial dimensions later. If the environment remains unchanged during the measurements, the channel stationarity allows to measure single trajectories sequentially and combine them to a radio channel map subsequently. In this section, we introduce the measurement procedure to build a two-dimensional radio channel map subsequently and briefly discuss the resulting map.

##### A. Sequential Measurement Approach

As shown in Fig. 1, the measurement track has an elongated shape with a long lower straight and a long upper straight, where the AGV moves counter-clockwise. Both straights are separated by a distance of 0.6 m. The surface of the AGV has a width of 44 cm and the AGV follows the line centered. The transmit antenna can be placed freely on the top of the AGV as illustrated in Fig. 3. Furthermore, there is an additional carrier surface (width of 92 cm) to extend the top surface of the AGV such that antenna positions next to the vehicle are measurable. The initial position of the antenna is in the middle between the two lanes. The antenna position remains unchanged during

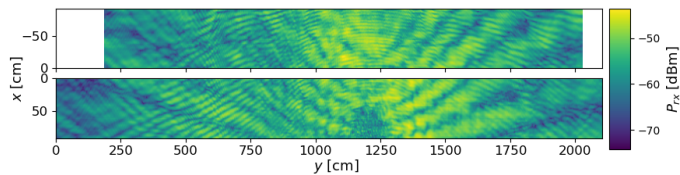


Fig. 4: Resulting radio environment maps for both straights around AP 2 after sequentially measuring the radio channel.

a measurement round. After a round is completed, the  $x$  position of the antenna is shifted by  $\Delta x$  on the surface towards the wall before the next round starts. This procedure was repeated until the outer edge of the carrier was reached. For the selection of  $\Delta x$ , a target correlation level between the lanes was set. A sufficient correlation is needed to align the individually measured lanes during post-processing. With an offset of  $\Delta x = 1$  cm per measurement round, a correlation coefficient of 0.96 for adjacent lanes results which is sufficient to align the lanes afterwards.

### B. Radio Channel Map Construction

After measuring the radio channel sequentially lane by lane, the measurement data is combined in a REM. Since the data of one lap is a contiguous time series, we first divide the lap so that the lower and upper straights are available individually. The resulting time series of the upper straight is then flipped because the AGV moves in the opposite direction here. In the next step, all receive power time series are sorted in ascending order according to their  $x$  coordinate. Starting from the lane with the smallest  $x$ , the single time series are aligned iteratively with the help of cross-correlation. For example, the second lane is aligned to the first lane. Then, the third lane is aligned to the second lane and so on. The high correlation between the lanes allows to find the constant offset per round originating from the slightly different measurement start. Since there is a small gap between the straights, this procedure is done for both straights separately. The resulting receive powers per coordinate are then illustrated as heat maps in Fig. 4. Note that the gap between the two maps does not coincide with the real distance but rather highlights that the two maps are created separately.

As a result of the described measurement methodology, two 0.92 m wide and over 18 m long receive power scans of the environment, measured from the AP, are created. The achieved spatial resolution is 10 mm in  $x$  and 0.8 mm in  $y$ . Visual inspection of this receive power map allows for some interesting conclusions. First of all, a wave propagation pattern around AP 2 in the corridor becomes clearly visible. AP 2 is approx. located at position (100cm, 1180cm) on the map. A shadowed area underneath the AP as well as a high receive power in close proximity to the receiving unit is observable. Further away from the access point, an interference pattern caused by multi-path propagation is clearly visible.

By looking at the power time series of the measurements only along the driving dimension, i.e., in the  $y$ -direction as it was shown in Fig. 2, large and fast changes of the received

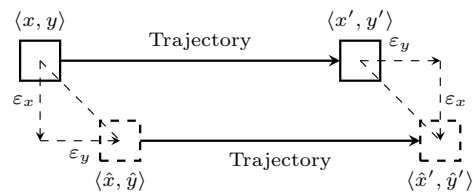


Fig. 5: Due to position errors  $\varepsilon_x$  and  $\varepsilon_y$ , the estimated position  $\langle \hat{x}, \hat{y} \rangle$  does not coincide with the true position  $\langle x, y \rangle$ . The future position based on the trajectory is thus false and a prediction error occurs.

power were visible. The measured radio map explains these occurrences. By driving on a horizontal line in  $y$ -dimension, the vehicle passes constructive and destructive interference positions. Depending on the  $x$ -coordinate of the lane, the angle between the interference stripes and the lane changes. Thus, the duration of how long a user experiences a constructive or destructive interference during the drive varies accordingly.

If we consider the usage of spatial channel information for predictions of the radio channel depending on the vehicle trajectory, one has to take the positioning uncertainty of the vehicle into account. Therefore, we investigate the influence of the positioning error on the predictions in the next section.

## V. IMPACT OF LOCALIZATION ERRORS

Considering the measured REM for channel predictions based on the planned trajectory of the vehicle, knowing the exact position of the AGV is essential. Assuming an error-free localization, the expected receive power is simply extracted from the map for a static environment. With this approach, the prediction error is theoretically independent of the prediction horizon along an arbitrary trajectory (and thus of the coherence time), but only depends on the localization error in  $x$  and  $y$  dimension as shown in Fig. 5. In a real system, the position of the vehicle must be estimated. Even though localization will improve in upcoming radio generations, there will inevitably be an error in the position estimation and the question arises how this error affects the channel prediction accuracy. Within the scope of this work, we investigate the impact of the localization error in two stages. First, a one-dimensional localization error  $\varepsilon_y$  in the direction of the vehicle's trajectory is considered. Second, the impact of localization errors  $\varepsilon_x$  and  $\varepsilon_y$  in both dimensions are investigated.

### A. One-dimensional Localization Error

For the one-dimensional case, we distinguish between a constant localization error and a possibly varying localization error along the direction of motion. Starting with the constant error, the receive power deviations between a position  $\langle x, y \rangle$  and the position  $\langle x, y + \varepsilon_y \rangle$  are evaluated. The difference  $E(x, y, \varepsilon_y) = |P_{rx}(x, y + \varepsilon_y) - P_{rx}(x, y)|$  is referred to as the prediction error at position  $\langle x, y \rangle$ . This is done for all possible positions  $\langle x, y \rangle$  in both maps and for different localization errors  $\varepsilon_y$ . As a result, there is an empirical prediction error distribution per localization error combined from both maps. Since a vehicle can move in positive and negative  $y$ -direction

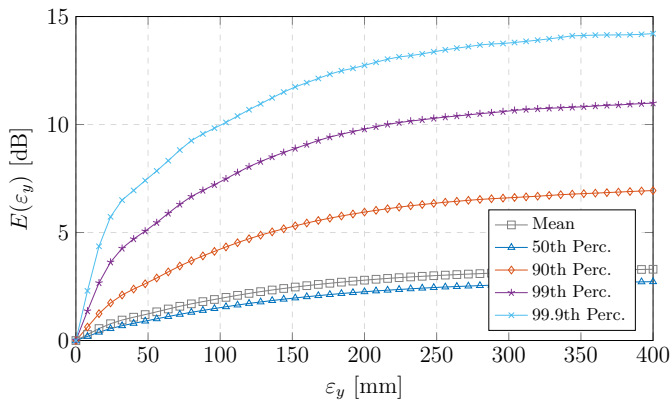


Fig. 6: Mean and percentiles of occurring prediction error distributions based on different one-dimensional, constant localization errors.

in our scenario, the absolute difference is evaluated. A positive error in one direction refers to a negative prediction error in the opposite direction.

From the empirical prediction error distributions, we determine percentiles and illustrate them in Fig. 6. There is a clear difference visible between the mean absolute error and higher percentiles, e.g., the 99% percentile, which are especially important in the context of URLLC applications. Depending on the prediction accuracy we want to achieve, we need to bound the localization error. As an example, if a probability of 99% for prediction errors smaller than 8 dB is targeted,  $\varepsilon_y$  has to be kept lower than 125 mm. From the results it is noteworthy that already a mislocalization of 10 cm can make the channel gain differ by 10 dB in this rather simple environment for a signal bandwidth of 80 MHz. To assess the measurement results, we refer to the localization performance achieved by a state-of-the-art localization based on a Light Detection And Ranging (LiDAR) sensor in [14]. The mean localization error was 4 cm and the maximum error is given with 12 cm for an indoor environment and a comparable speed. With this accuracy, 90% of the prediction errors are not exceeding 5 dB.

In addition to the constant localization error, we investigate a localization error that can vary but is limited by a maximum error  $\varepsilon_{y,\max}$ . The intention is that a localization error is typically not fixed but follows a bounded random process. The maximum and thus worst prediction error does not necessarily occur at the maximum localization error, but also occurs at smaller localization errors. Please note, that this leads to a worst-case evaluation. Therefore, the maximum prediction error  $E_{\max}$  between position  $\langle x, y \rangle$  and position  $\langle x, y + \varepsilon_{y,\max} \rangle$  is evaluated, i.e., we determine

$$E_{\max}(x, y, \varepsilon_y) = \max_{\varepsilon_y \in \Sigma_y} (|P_{\text{rx}}(x, y + \varepsilon_y) - P_{\text{rx}}(x, y)|) \quad (2)$$

with  $\Sigma_y = \{0, \dots, \varepsilon_{y,\max}\}$  [mm] for all possible positions  $\langle x, y \rangle$  in the maps. This again results in new maximum prediction error distributions per localization error that we evaluated in Fig. 7. There, the varying localization error is compared with the constant localization error. For errors exceeding 50 mm, the variable error causes higher prediction errors.

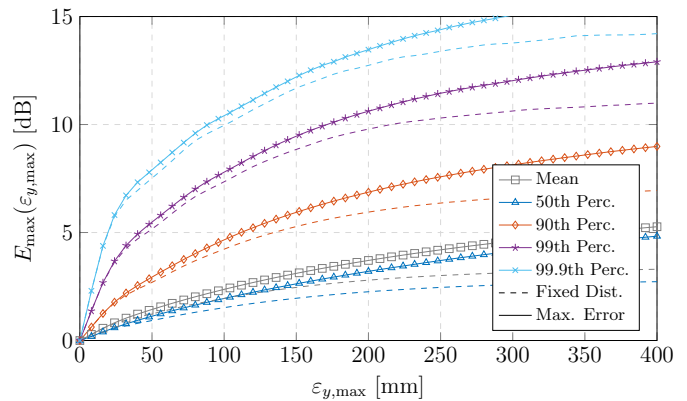


Fig. 7: Mean and percentiles of occurring prediction error distributions based on different one-dimensional, bounded localization errors.

## B. Two-dimensional Localization Error

Next, the radio map from Sec. IV is used to consider the impact of localization errors in both dimensions on the prediction error. This is relevant for the following two reasons: 1) In a real scenario, an AGV can move in all directions. Thereby, both  $x$  and  $y$  coordinates change and are to be estimated. 2) Both coordinates are subject to the localization error.

In this work, we assume that the localization error behaves identical in both dimension. Sec. V-A shows that the maximum prediction error occurs with variable localization error. Since we focus on the maximum and thus worst prediction error, we determine the maximum receive power deviation in a bounded area around a position  $\langle x, y \rangle$ , i.e., we determine

$$E_{\max}(x, y, \varepsilon_x, \varepsilon_y) = \max_{\varepsilon_x \in \Sigma_x, \varepsilon_y \in \Sigma_y} (|P_{\text{rx}}(x + \varepsilon_x, y + \varepsilon_y) - P_{\text{rx}}(x, y)|) \quad (3)$$

with  $\Sigma_x = \Sigma_y = \{-\varepsilon_{x,\max}, \dots, \varepsilon_{x,\max}\}$  [mm] for all possible positions  $\langle x, y \rangle$  in the map.

Note again, that this evaluation results in a worst-case assessment for the maximum possible errors. The impact of the two-dimensional localization error on the prediction error is shown in Fig. 8. For comparison, the maximum one-dimensional error curves are presented. The mean as well as percentiles indicate a clear increase of the prediction error by approximately 6 dB to 7 dB. The interference patterns in the radio map shown in Fig. 4 provide the explanation for the deviation. High prediction errors occur if the direction of the resulting localization error is perpendicular to the interference stripes. By looking at horizontal errors  $\varepsilon_y$  as it was done in Sec. V-A, the angles between trajectory and interference stripes do not cause the maximum possible receive power deviations. The radio channel shows a significantly different spatial variation depending on the spatial direction. Thus, we conclude that the directionality of the localization error has a large impact on the prediction error depending on the environment geometry. Considering the localization performance from [14], the maximum possible prediction errors are much

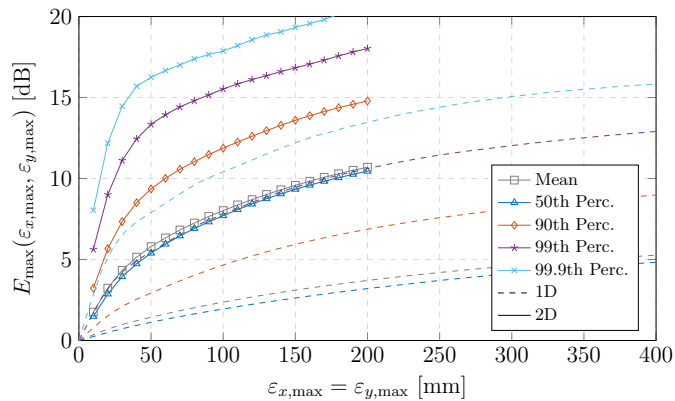


Fig. 8: Mean and percentiles of occurring prediction error distributions based on different two-dimensional, bounded localization errors.

higher compared to the one-dimensional case. Even the good mean localization performance of 4 cm makes that 50 % of the maximum prediction errors will exceed 5 dB and the highest prediction errors will exceed 17 dB for this accuracy.

## VI. CONCLUSION

In this work, an indoor measurement campaign for analyzing REMs in the context of channel predictions was presented. With the measurement system shown, the assumption of spatio-temporal stationarity of the radio channel was verified in the whole static measurement environment. In addressing the research question of whether REMs are usable for channel prediction, the results show that this approach is promising in static environments.

Even though the stationarity shown motivates the utilization, the performance of this prediction methodology is limited by the localization accuracy. To quantify the impact of the localization, we made a worst-case evaluation of the measurements by looking at the maximum occurring prediction errors. Even for localization errors of few centimeters only, the prediction error can exceed 10 dB, emphasizing the need for accurate localization to bound the prediction error. However, a position-dependent and direction-dependent spatial variation of the receive power is observable. We therefore conclude that the required localization accuracy is varying depending on the channel variation through the environment. This finding relaxes the localization requirements in regions where the spatial correlation is detected to be high.

Based on the methods and results presented, a variety of future investigations arise. For URLLC, very accurate predictions are required and hence REMs with very high resolution. However, measuring at this resolution is a hindrance to practical application. With the presented high-resolution REM available, we can study the impact of reducing the resolution on the prediction error. Furthermore, we want to dispense with the assumption of a static environment and investigate the usability of REMs for channel predictions in an environment that experiences static and dynamic changes. Initial experiments show that the impact of moving objects in the

environment is spatially limited. Inspired by this observation, the detection and identification of occurring non-stationarities, i.e., of environment deviations, is thereby a topic we will investigate with our measurement setup. In this work, we focused on the evaluation of wideband signal powers. In the future, we will include the frequency spectrum information per position into our analysis.

## ACKNOWLEDGMENT

This work was supported by the German Federal Ministry of Education and Research (BMBF) as part of the project "AI4Mobile" under grant 16KIS1177. It was also funded by the German Research Foundation (DFG, Deutsche Forschungsgemeinschaft) as part of Germany's Excellence Strategy – EXC 2050/1 – Project ID 390696704 – Cluster of Excellence "Centre for Tactile Internet with Human-in-the-Loop" (CeTI) of Technische Universität Dresden.

## REFERENCES

- [1] E. A. Oyekanlu *et al.*, "A Review of Recent Advances in Automated Guided Vehicle Technologies: Integration Challenges and Research Areas for 5G-Based Smart Manufacturing Applications," *IEEE Access*, vol. 8, 2020.
- [2] A. Frotzschner *et al.*, "Requirements and current solutions of wireless communication in industrial automation," in *2014 IEEE International Conference on Communications Workshops (ICC)*, 2014.
- [3] A. TraBl *et al.*, "Outage prediction for ultra-reliable low-latency communications in fast fading channels," *J Wireless Com Network*, vol. 92, no. 6, 2021.
- [4] H. Wymeersch *et al.*, "Integration of Communication and Sensing in 6G: a Joint Industrial and Academic Perspective," in *2021 IEEE 32nd Annual International Symposium on Personal, Indoor and Mobile Radio Communications (PIMRC)*, 2021.
- [5] H. Zou *et al.*, "Adversarial Learning-Enabled Automatic WiFi Indoor Radio Map Construction and Adaptation With Mobile Robot," *IEEE Internet of Things Journal*, vol. 7, no. 8, 2020.
- [6] K. Mendes, F. Lemic, and J. Famaey, "Small UAVs-supported Autonomous Generation of Fine-grained 3D Indoor Radio Environmental Maps," *CoRR*, vol. abs/2111.03451, 2021. [Online]. Available: <https://arxiv.org/abs/2111.03451>
- [7] H. Suzuki and A. Mohan, "Measurement and prediction of high spatial resolution indoor radio channel characteristic map," *IEEE Transactions on Vehicular Technology*, vol. 49, no. 4, 2000.
- [8] C. Zhou *et al.*, "Exploiting Fingerprint Correlation for Fingerprint-Based Indoor Localization: A Deep Learning Based Approach," *IEEE Transactions on Vehicular Technology*, vol. 70, no. 6, 2021.
- [9] R. Zhong *et al.*, "Path Design and Resource Management for NOMA enhanced Indoor Intelligent Robots," *CoRR*, vol. abs/2011.11745, 2020. [Online]. Available: <https://arxiv.org/abs/2011.11745>
- [10] J. Webber *et al.*, "Machine Learning-based RSSI Prediction in Factory Environments," in *2019 25th Asia-Pacific Conference on Communications (APCC)*, 2019.
- [11] F. Burmeister *et al.*, "Measuring Time-Varying Industrial Radio Channels for D2D Communications on AGVs," in *IEEE Wireless Communications and Networking Conference*, 2021.
- [12] M. Danneberg *et al.*, "Online Wireless Lab Testbed," in *2019 IEEE Wireless Communications and Networking Conference Workshop (WCNCW)*, 2019, pp. 1–5.
- [13] F. Burmeister, Z. Li, and I. Bizon, "High-resolution radio environment map data set for indoor office environment," 2022. [Online]. Available: <https://dx.doi.org/10.21227/waxd-9525>
- [14] E. Sánchez *et al.*, "High precision indoor positioning by means of LiDAR," in *2019 DGON Inertial Sensors and Systems (ISS)*, 2019.